Viscoelastic Modeling of Tidal Stress on Satellites with SatStressGUI: Now With Polar Wander

D. Alex Patthoff[1,2], R.T. Pappalardo[2], A. Ismailyan[3,2], P. Sinclair[4,2], J. B. Li[5,2], B. Ayton[6,2], D. Dubois[7,2], J. P. Kay[8], S. A. Kattenhorn[9]

[1]Planetary Science Institute (apatthof@psi.edu), [2]Jet Propulsion Laboratory, California Institute of Technology, [3]University of California, Irvine, [4]University of New Mexico, [5]California Institute of Technology, [6]Massachusetts Institute of Technology, [7]University of Versailles St. Quentin, [8]University of Illinois at Chicago, [9]University of Alaska, Anchorage

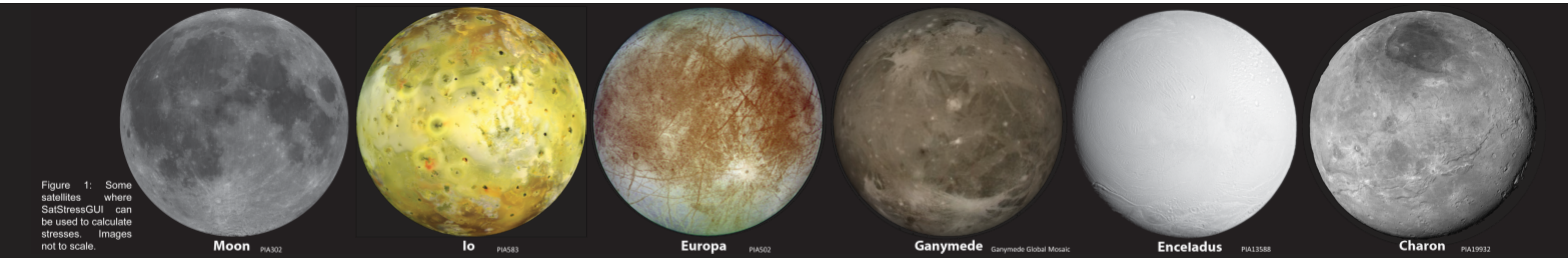

Figure 1: Some satellites where SatStressGUI can be used to calculate stresses. Images not to scale.

Introduction

Icy and rocky satellites of our solar system display a diverse range of geological deformation on their surfaces (Figure 1). Some moons appear old and heavily cratered showing little evidence for recent tectonism while other moons are sparsely cratered and young. The deformation can take the form of small cracks in the surface, large double ridges that can extend for thousands of km, and mountain ranges that can reach heights of several km. A key source of stress that can deform satellite surfaces is the diurnal tidal deformation of the moons as they orbit their parent planets. Other secular sources of global-scale stress include: volume change induced by the melting or freezing of a subsurface liquid layer, change in the orbital parameters of the moon, a tilt in the axis of rotation (obliquity), or rotation of the outer shell of the satellite relative to the rest of the body (nonsynchronous rotation [NSR] or true polar wander). We turn to computer modeling to correlate observed structural features to the possible stresses that created them. A variety of modeling programs exist and generally assume a thin ice shell and/or a multi-layered viscoelastic satellite. The program SatStress (Wahr et al.,2009), computes diurnal and NSR stresses on a satellite. It was later modified into a more user-friendly version with a graphic user interface (SatStressGUI) by Kay & Kattenhorn (2010). This implementation assumes a 4-layer viscoelastic body and is able to calculate stresses resulting from diurnal tides, NSR, and ice shell thickening. Here we demonstrate our recent enhancements to SatStressGUI, including the ability to generate cycloid-like lineaments, calculate stresses resulting from obliquity, and more efficiently batch process data.

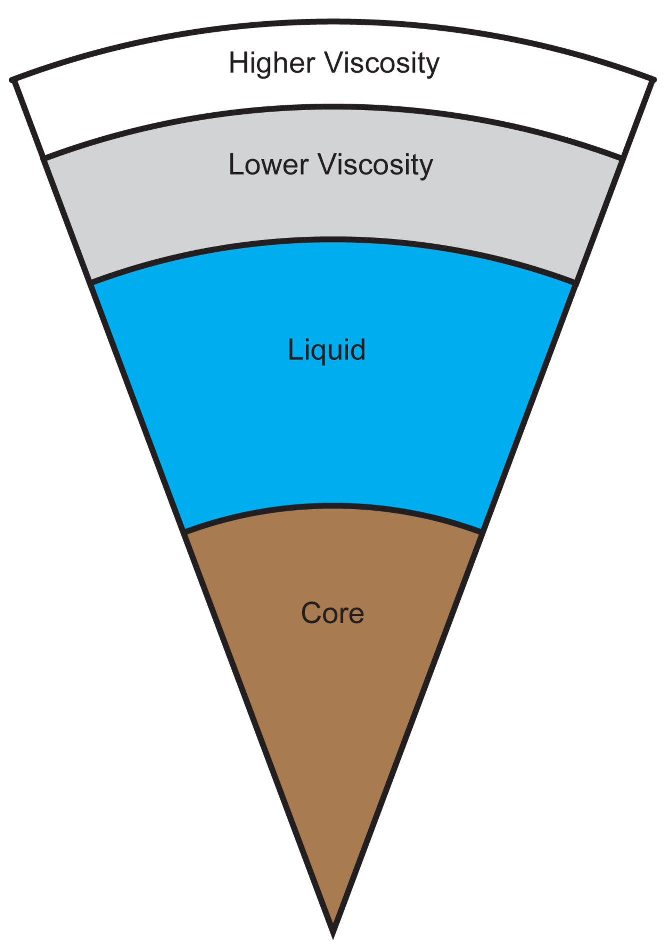

1) Build a Satellite and Select Stresses

The 4 layers used by SatStressGUI consists of 2 outer layers subdivided into a top more viscous layer and a lower less viscous layer (Figures 2 and 3). The third layer must be liquid, and the inner-most layer is the core or combined core and mantle. The user inputs the "Planet Mass," (mass of the parent planet), eccentricity of the satellite, and the semimajor axis of the orbit. There is an option to set a NSR period or, if no NSR is desired, this can be set to "infinity." The user defines the name, density, Young's modulus, Poisson's ratio, thickness, and viscosity of each layer. A tensile strength can be defined to generate lineaments on the final plots to show where fractures are predicted to occur. All calculations, except the ice shell thickening and polar wander stresses, are preformed using the viscoelastic model. The ice shell thickening calculations assumes an instantaneous homogenous change in thickness and the polar wander is assumed to be in an elastic medium. We have updated the diurnal and NSR Love number calculator following Zábranová et al (2009) and Dahlen and Tromp (1998). We have added the ability to calculate obliquity stresses following the model of Jara-Orué and Vermeersen, (2011) and polar wander following the model of Matsuyama and Nimmo (2008).

Figure 2: Generalized 4-layer interior structure of a satellite. For icy satellites this can be divided into a high viscosity and cold outer ice layer, less viscous and warm inner ice layer, global water ocean, and a rocky interior core.

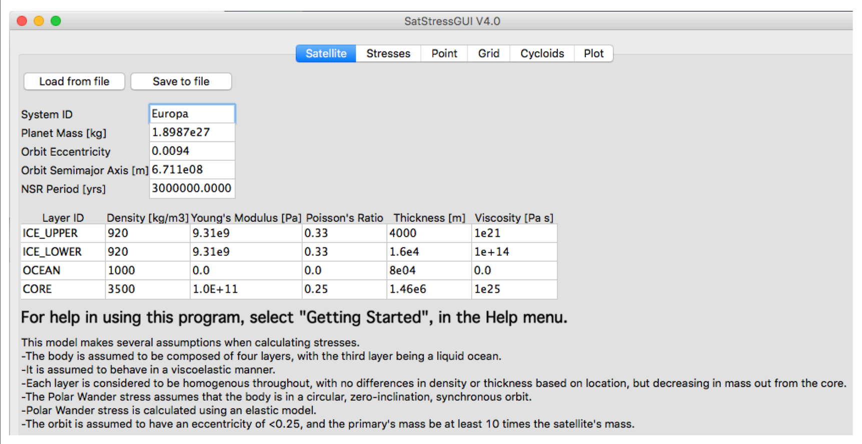

Figure 3: Screen capture of SatStressGUI showing a generalized Europa model with a 3 Myr NSR period. All parameters can be modified to best fit other satellites and their constitutive properties of ice or rock layers.

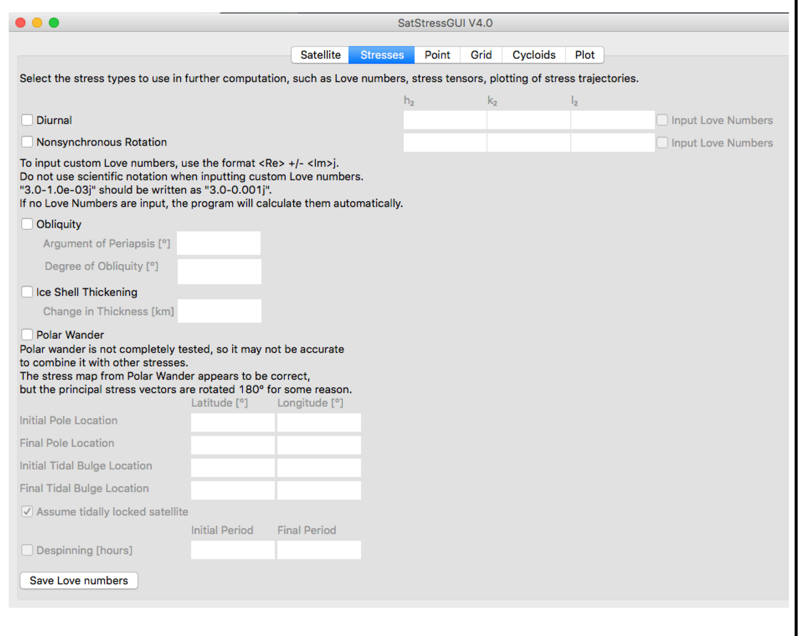

Figure 4: Screen capture of the stresses input tab. Here the user has SatStressGUI calculate Love numbers (default) or inputs their own. The user also selects the desired stress or combination of stresses to be calculated.

2) Plotting stresses and cycloids.

Cycloidal structures can be modeled with the assumption that one arc is created each orbit (Hoppa et al., 1999). The user specifies an initial yield strength, propagation strength, propagation speed, starting location, and propagation direction as shown in Figure 5.

Plots of stresses (Figure 6) can be displayed for a variety of projections including: simple cylindrical, Mercator, orthographic, Miller cylindrical, and polar. Plots can be exported to an ArcGIS environment (shape file) or saved as tiff files. The user can observe how stresses change throughout an orbit.

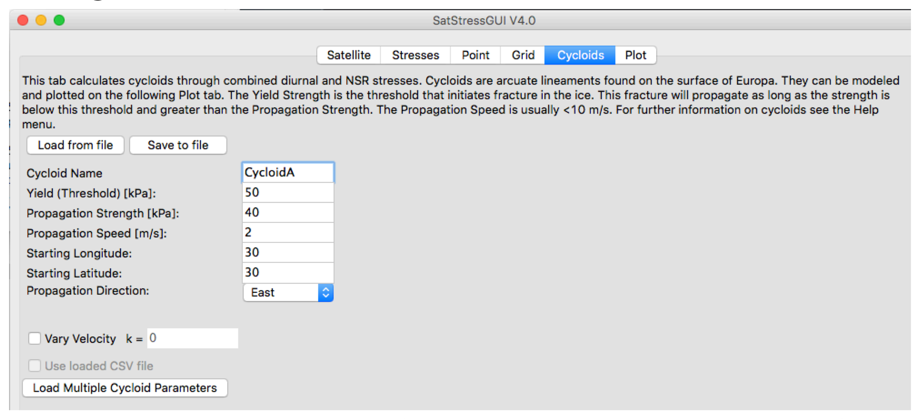

Figure 5: Screen capture of SatStressGUI showing user-defined inputs for cycloid generation. Propagation strength should be less than or equal to the initial yield strength. The "vary speed" function is currently in development.

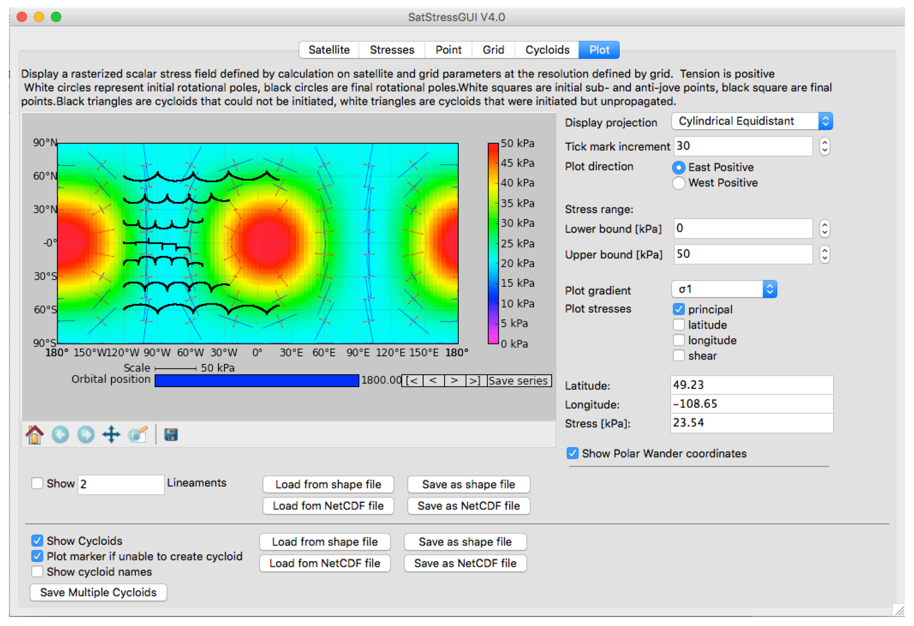

Figure 6: Screen capture of the plotting functions for SatStressGUI. User can specify the stress range, and which stress representation to plot (σ1, σ3, average stress, or differential stress). Tick marks show the vector of the chosen stress. Here we show the results from a sample Europa with modeled cycloids.

3) Sample outputs.

Here we show preliminary results for a sample Europa model showing the stresses SatStressGUI is able to calculate and display.

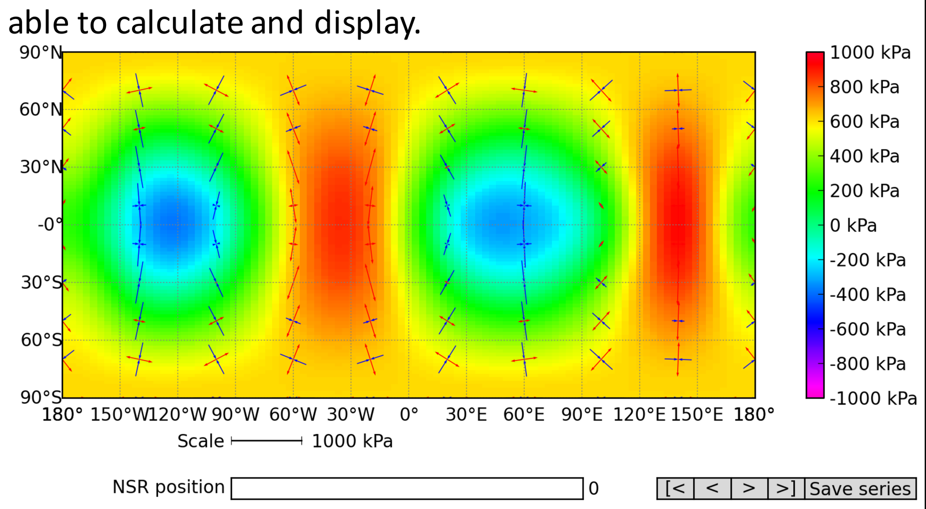

Figure 7: Nonsynchronous rotation. Here we show a sample output of the stresses created by nonsynchronous rotation on a sample Europa. The magnitude is dependent on the structure of the ice shell and period of rotation.

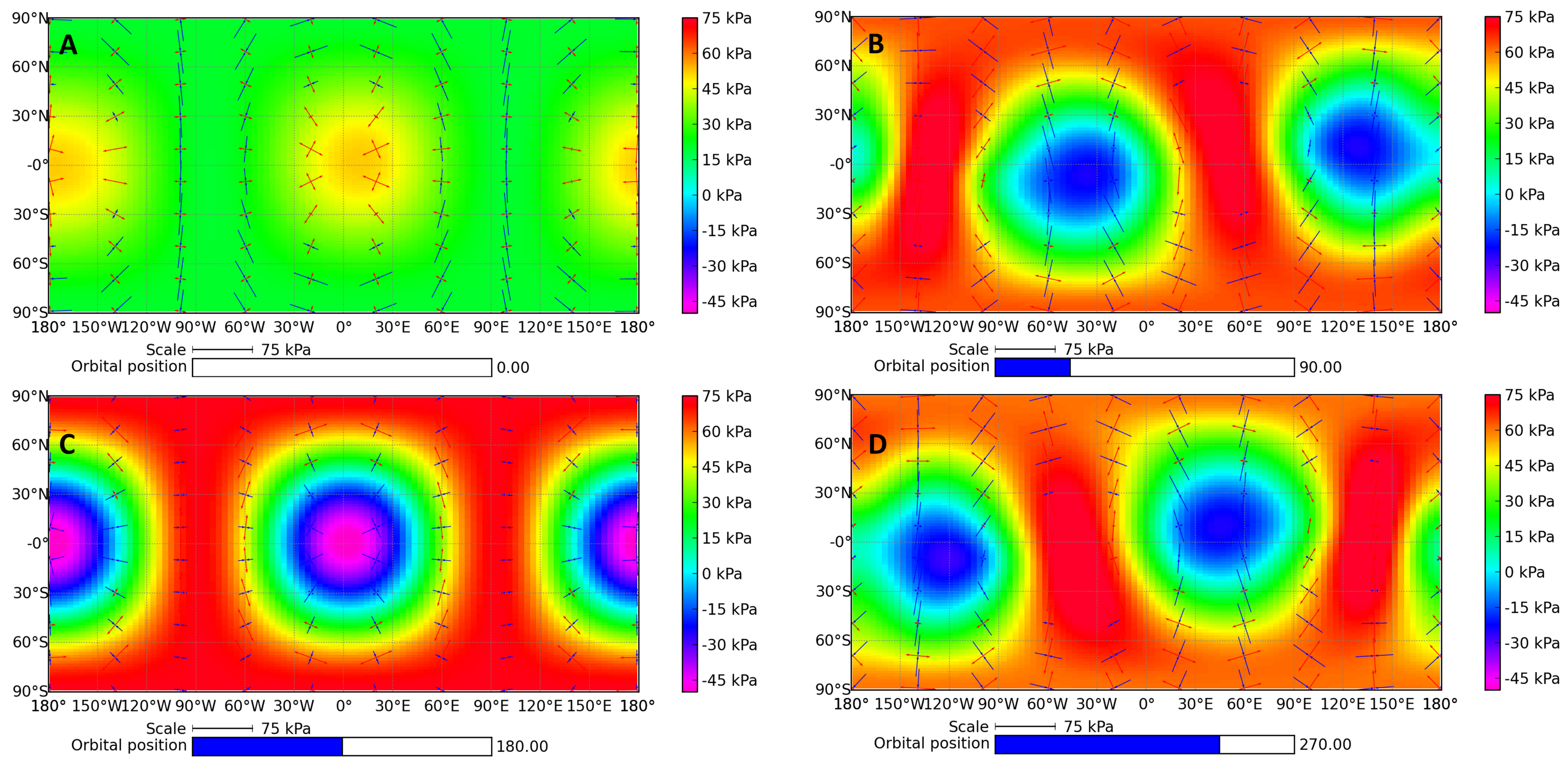

Figure 8: Figure showing stresses resulting form diurnal tidal stresses and 0.25° of obliquity over 1 orbit. A) periapsis, B) 90° past periapsis, C) apoapsis, and D) 90° past apoapsis.

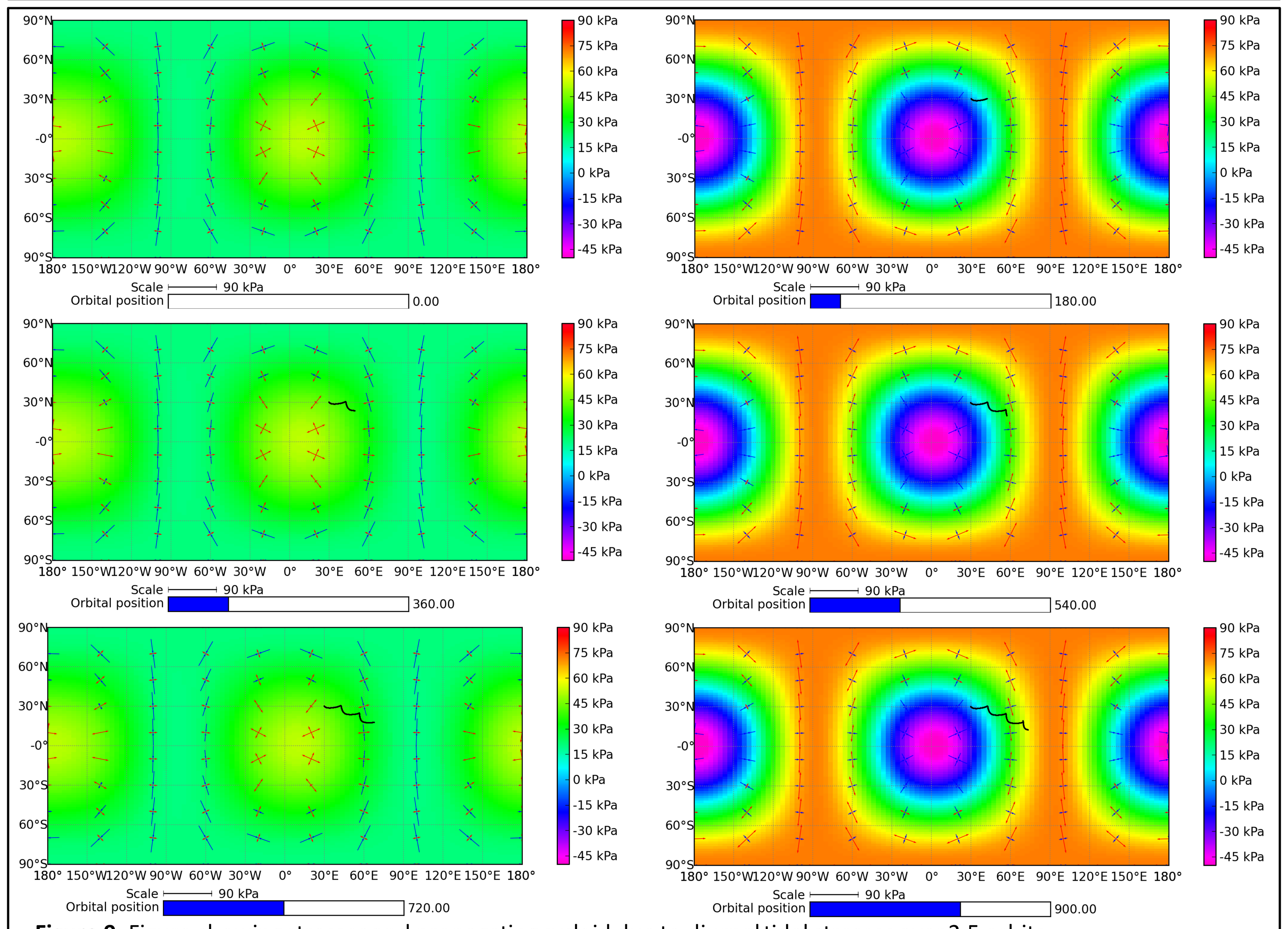

Figure 9: Figure showing stresses and propagating cycloid due to diurnal tidal stresses over 2.5 orbits.

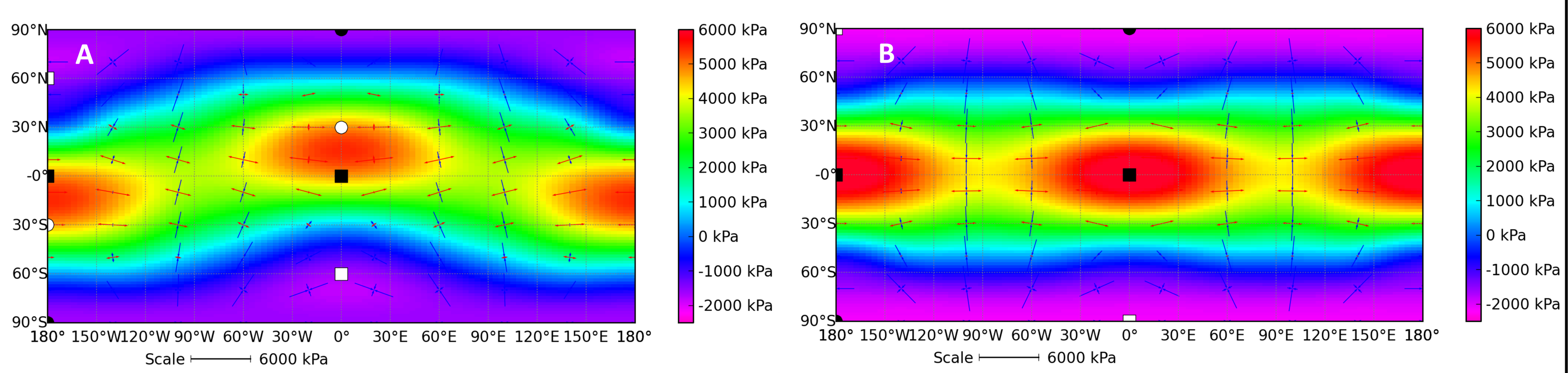

Figure 10: Figure showing polar wander stresses resulting from A) 30° of polar wander and B) 90° of polar wander. The rotational poles are marked by circles and the sub- and anti-jove points are marked with triangles. Black marks denote final positions and white marks are initial positions.

References

Dahlen & Tromp (1998). Theoretical global seismology. Princeton University Press; **Hoppa et al. (1999).** Formation of cycloidal features on Europa. Science, 285, 1899-1902; **Jara-Orué & Vermeersen (2011).** Effects of low-viscous layers and a non-zero obliquity on surface stresses induced by diurnal tides and non-synchronous rotation: The case of Europa. Icarus, 215, 417-438; **Kay & Kattenhorn (2010).** An open-source GUI for calculating icy moon tidal stresses using SatStress. 41st LPSC, Abstract 2046; **Matsuyama and Nimmo (2008).** Tectonic patterns on reoriented and despun planetary bodies. *Icarus, 195*, 459-473; **Wahr et al. (2009).** Modeling stresses on satellites due to nonsynchronous rotation and orbital eccentricity using gravitational potential theory. Icarus, 200, 188-206; **Zábranová, et al. (2009);** Matrix pseudospectral method for elastic tides modeling. Mission and Passion: Science; Prague, 243-260.